MucosalImmunology www.nature.com/mi

ARTICLE OPEN

Phosphatidylinositol 3-kinase p110δ drives intestinal fibrosis in SHIP deficiency

Young Lo[1], Jean Philippe Sauve[1], Susan C. Menzies[1], Theodore S. Steiner[2] and Laura M. Sly[1]

Crohn's disease is an immune-mediated disease characterized by inflammation along the gastrointestinal tract. Fibrosis requiring surgery occurs in one-third of people with Crohn's disease but there are no treatments for intestinal fibrosis. Mice deficient in the SH2 domain-containing inositolpolyphosphate 5′-phosphatase (SHIP), a negative regulator of phosphatidylinositol 3-kinase (PI3K) develop spontaneous Crohn's disease-like intestinal inflammation and arginase I (argI)-dependent fibrosis. ArgI is up-regulated in SHIP deficiency by PI3Kp110δ activity. Thus, we hypothesized that SHIP-deficient mice develop fibrosis due to increased PI3Kp110δ activity. In SHIP-deficient mice, genetic ablation or pharmacological inhibition of PI3Kp110δ activity reduced intestinal fibrosis, including muscle thickening, accumulation of vimentin$^+$ mesenchymal cells, and collagen deposition. PI3Kp110δ deficiency or inhibition also reduced ileal inflammation in SHIP-deficient mice suggesting that PI3Kp110δ may contribute to inflammation. Targeting PI3Kp110δ activity may be an effective strategy to reduce intestinal fibrosis, and may be particularly effective in the subset of people with Crohn's disease, who have low SHIP activity.

Mucosal Immunology (2019) 12:1187–1200; https://doi.org/10.1038/s41385-019-0191-z

INTRODUCTION

Inflammatory bowel disease (IBD) is an immune-mediated disease characterized by inflammation along the gastrointestinal tract.[1] One in 150 people in North America have IBD and the incidence of disease is increasing in developed countries.[1] Crohn's disease (CD) is a subtype of IBD, which is characterized by discontinuous inflammation that can occur anywhere along the gastrointestinal tract.[2] CD-associated inflammation is transmural and can cause bowel perforations.[2] In addition, approximately one in three people with CD develops strictures within 10 years of diagnosis that require surgery to remove the diseased bowel.[3] Intestinal resection or stricturoplasty is ultimately necessary in up to 75% of CD patients during the course of their disease.[4] Moreover, people that develop fibrosis are at increased risk of recurrence.[5]

Fibrosis can be considered an uncontrolled healing response.[6] It follows the distribution and location of inflammation in people with CD and likely occurs downstream of chronic inflammation due to repeated cycles of injury and repair.[7] Biological therapy, including blocking antibodies against TNFα, is very effective at inducing and maintaining remission in people with CD.[8] However, early studies report that blocking inflammation with biologics did not reduce the incidence of fibrosis or surgery in people with CD, suggesting that subclinical inflammation may be sufficient to induce fibrotic pathology in some individuals.[9] Early introduction of biological therapy may be more effective at reducing fibrosis and some studies suggest that the incidence of fibrosis has been reduced by the use of biologics, but still remains significant.[9,10] At risk populations include the 30% of people with CD, who experience loss of treatment efficacy over time[11,12]; pediatrics patients, who are treated by a step-up approach to therapy[13]; and people, who have already developed fibrosis.[7] Identification of distinct fibrotic mechanisms may permit development of urgently needed therapeutic approaches to target fibrosis directly.[4,6]

Class I phosphatidylinositol 3-kinases (PI3Ks) regulate multiple intracellular signaling pathways and biological processes, including inflammation.[14] PI3K phosphorylates phosphatidylinositol 4,5-bisphoshophate ($PI(4,5)P_2$) to generate $PI(3,4,5)P_3$, a critical second messenger.[15] PI3K consists of a regulatory subunit (p85α, p85β, p55α, or p55γ) and a catalytic subunit (p110α, p110β, p110γ, or p110δ).[15] The isoforms of the catalytic subunit perform distinct functions within cells.[15] Guo et al.[16] created mice with a point mutation (D→A) in the active site of PI3Kp110δ. These mice, designated $PI3Kp110\delta^{D910A/D910A}$, have no p110δ catalytic activity but retain normal protein levels of all p110 catalytic subunit isoforms.[16] $PI3Kp110\delta^{D910A/D910A}$ mice have been reported to develop mild colitis beginning at 8 week of age,[17] but colitis is dependent on the environment and does not occur in our mouse colony.[18]

PI3K signaling is regulated by lipid phosphatases. The SH2 domain-containing inositolpolyphosphate 5′-phosphatase (SHIP) is a hematopoetic-specific 5′ lipid phosphatase, which regulates PI3K-mediated cell signaling and is important in type II immune responses in mast cells and macrophages.[15] Mice deficient in SHIP suffer from chronic inflammatory pathologies in the lung and gut.[15] In the gut, SHIP-deficient mice develop spontaneous CD-like intestinal inflammation that occurs in the distal ileum and is present in all mice by 6 weeks of age.[19,20] We have reported that inflammation is accompanied by intestinal fibrosis including muscle thickening and increased collagen deposition, which is dependent on the enzyme, arginase I (argI).[19] ArgI is induced in macrophages by treatment with IL-4, leading to the generation of canonical alternatively activated macrophages, M(IL-4).[18]

[1]Division of Gastroenterology, Department of Pediatrics, BC Children's Hospital Research Institute, University of British Columbia, Vancouver, BC, Canada and [2]Division of Infectious Diseases, Department of Medicine, BC Children's Hospital Research Institute, University of British Columbia, Vancouver, BC, Canada
Correspondence: Laura M. Sly (laurasly@mail.ubc.ca)

Received: 6 December 2018 Revised: 23 June 2019 Accepted: 15 July 2019
Published online: 29 July 2019

Moreover, we have found IL-4-mediated induction of arg1 requires the p110δ catalytic subunit of Class IA PI3K.[18,21]

Thus, we hypothesized that PI3Kp110δ activity drives intestinal fibrosis in SHIP$^{-/-}$ mice. Herein, we present genetic and biochemical evidence to demonstrate a critical role for PI3Kp110δ in the development of fibrosis in SHIP$^{-/-}$ mice. Further, we show that targeting PI3Kp110δ and fibrosis ameliorates the development of spontaneous CD-like intestinal inflammation in SHIP-deficient mice.

RESULTS

p110δ regulates arg1 expression and activity

To interrogate whether the intestinal fibrosis that develops in SHIP$^{-/-}$ mice is driven by PI3Kp110δ activity, SHIP$^{-/-}$ mice were crossed with mice expressing a catalytically inactive form of PI3Kp110δ, PI3Kp110δ$^{D910A/D910A}$ (p110δ$^{DA/DA}$). We first asked whether IL-4-mediated arg1 induction was compromised in macrophages from mice deficient in p110δ activity. IL-4 induced arg1 protein expression in macrophages from SHIP$^{+/+}$p110δ$^{+/+}$, SHIP$^{+/+}$p110δ$^{DA/DA}$, and SHIP$^{-/-}$p110δ$^{+/+}$ mice, but was compromised in macrophages from SHIP$^{-/-}$p110δ$^{DA/DA}$ mice (Fig. 1a). Arginase activity was present in all genotypes of mice but was significantly higher in SHIP$^{-/-}$ mice (Fig. 1b); and was significantly lower in macrophages from SHIP$^{+/+}$p110δ$^{DA/DA}$ and SHIP$^{-/-}$p110δ$^{DA/DA}$ mice relative to their p110δ$^{+/+}$ littermates (Fig. 1b).

Arginase activity was measured in full-thickness ileal tissue homogenates from mice of each genotype at 4 weeks, prior to the onset of intestinal inflammation, 8 weeks, and 12 weeks of age. At 4 weeks of age, arginase activity was significantly lower in tissues from SHIP$^{-/-}$p110δ$^{DA/DA}$ mice compared to their SHIP$^{-/-}$p110δ$^{+/+}$ littermates (Fig. 1c). At 8 and 12 weeks of age, SHIP$^{-/-}$p110δ$^{+/+}$ mice had higher levels of arginase activity in their ilea compared to either of the healthy control mice, SHIP$^{+/+}$p110δ$^{+/+}$ or SHIP$^{+/+}$p110δ$^{DA/DA}$ mice. Importantly, the SHIP$^{-/-}$p110δ$^{DA/DA}$ mice had significantly lower arginase activity in the ileum compared to the SHIP$^{-/-}$p110δ$^{+/+}$ mice (Fig. 1c). Ileal tissue cross-sections were stained by immunofluorescence for arg1 (red) and Ym1 (a marker of murine M(IL-4); green) and counterstained with DAPI. At all ages, healthy control mice (SHIP$^{+/+}$p110δ$^{+/+}$ and SHIP$^{+/+}$p110δ$^{DA/DA}$) expressed low baseline levels of arg1 primarily in the muscle layer and submucosa (Fig. 1d). In contrast, SHIP$^{-/-}$p110δ$^{+/+}$ mice had more arg1^{+} cells in the muscle layers and submucosa at all ages, which were lower in SHIP$^{-/-}$p110δ$^{DA/DA}$ mice (Fig. 1d). Ym1 expression was also higher in SHIP$^{-/-}$p110δ$^{+/+}$ mice compared to healthy control mice, particularly evident in 4-week-old mice and; like arg1 expression, the number of Ym1-expressing cells was lower in SHIP$^{-/-}$p110δ$^{DA/DA}$ mice compared to SHIP$^{-/-}$p110δ$^{+/+}$ mice (Fig. 1d).

p110δ regulates gross pathology and histological damage in SHIP$^{-/-}$ mice

To determine whether p110δ activity contributes to gross and histopathology in SHIP$^{-/-}$ mice, we examined ilea from 4-, 8-, and 12-week-old SHIP$^{+/+}$p110δ$^{+/+}$, SHIP$^{+/+}$p110δ$^{DA/DA}$, SHIP$^{-/-}$p110δ$^{+/+}$, and SHIP$^{-/-}$p110δ$^{DA/DA}$ mice. Ilea from 4-week-old mice appeared healthy with no gross signs of muscle thickening or redness (Fig. 2a). Ilea from the control mice, SHIP$^{+/+}$p110δ$^{+/+}$ and SHIP$^{+/+}$p110δ$^{DA/DA}$, also looked healthy at 8 and 12 weeks of age. However, ilea from 8- and 12-week-old SHIP$^{-/-}$p110δ$^{+/+}$ mice were thickened with red patches, whereas the ilea from 8- and 12-week-old SHIP$^{-/-}$p110δ$^{DA/DA}$ mice had dramatically reduced gross pathology (Fig. 2a). To characterize the structure and health of the ileum in each mouse genotype, ileal cross-sections were stained with H&E. The healthy control mice, SHIP$^{+/+}$p110δ$^{+/+}$ and SHIP$^{+/+}$p110δ$^{DA/DA}$, did not have histological evidence of disease at any age (Fig. 2b). Among the 4-week-old SHIP$^{-/-}$p110δ$^{+/+}$ group, two of six mice, including one shown, had modest enlargement of the ileum and muscle thickening (Fig. 2b, top, 3rd panel). In contrast, none of the 4-week-old SHIP$^{-/-}$p110δ$^{DA/DA}$ mice showed histological damage or evidence of muscle thickening. At 8 and 12 weeks of age, the distal ilea from all SHIP$^{-/-}$p110δ$^{+/+}$ mice were dramatically enlarged with thick muscle layers, and had goblet cell hyperplasia and hypertrophy, immune cell infiltrates and aggregates throughout the gut wall, and irregular crypt-villus architecture (Fig. 2b, 3rd column). Notably, ilea from the SHIP$^{-/-}$p110δ$^{DA/DA}$ mice were smaller, with thinner muscle layers, and reduced damage to crypt-villus architecture (Fig. 2b, 4th column).

Lung pathology was also examined in mice from each genotype because SHIP$^{-/-}$ mouse lungs display inflammatory pathology.[22] SHIP$^{-/-}$ mice lungs are enlarged with patchy white discoloration. The lungs from PI3Kp110δ$^{DA/DA}$ were also enlarged and the gross appearance of the SHIP$^{-/-}$ mouse lungs was not improved by p110δ deficiency (Suppl. Fig. 1a). Cross-sections of the right lobe of lungs from male mice were stained with Masson's trichrome. SHIP$^{+/+}$p110δ$^{+/+}$ (wild type) and SHIP$^{+/+}$p110δ^{DADA} (p110δ deficient control) lungs appeared healthy (Supplementary Fig. 1b). Lungs from SHIP$^{-/-}$p110δ$^{+/+}$ mice show immune cell infiltration and abundant staining for collagen (blue), which was dramatically improved by p110δ deficiency (Supplementary Fig. 1b).

p110δ deficiency reduces ileal fibrosis in SHIP$^{-/-}$ mice

Muscle thickness was measured in mice. SHIP$^{+/+}$PI3Kp110δ$^{+/+}$ and SHIP$^{+/+}$PI3Kp110δ$^{DA/DA}$ mice had thin muscle layers (muscularis and serosa) at all ages, whereas muscle layers were significantly thicker in SHIP$^{-/-}$PI3Kp110δ$^{+/+}$ mice (Fig. 3a). Ilea from 4- and 8-week-old SHIP$^{-/-}$ mice that were also deficient in PI3Kp110δ (SHIP$^{-/-}$PI3Kp110δ$^{DA/DA}$) had significantly thinner ileal muscle layers compared to their SHIP$^{-/-}$PI3Kp110δ$^{+/+}$ counterparts. This difference was not seen in mice at 12 weeks of age, which may be because the muscle is not as dramatically affected in 12-week-old SHIP$^{-/-}$PI3Kp110δ$^{+/+}$ mice.

Collagen was also measured in ileal tissues using the Sircol assay. No differences were noted in 4-week-old mice (Fig. 3b). At 8 and 12 weeks of age, the SHIP$^{-/-}$PI3Kp110δ$^{+/+}$ mice (disease control) had high amounts of soluble collagen in their distal ilea, whereas the SHIP$^{-/-}$PI3Kp110δ$^{DA/DA}$ mice had significantly lower amounts of soluble collagen (Fig. 3b). Fixed ileal tissue sections were also stained with Masson's trichrome (Fig. 3c). In the SHIP$^{-/-}$PI3Kp110δ$^{+/+}$ mice ilea, collagen was deposited mainly in the submucosa, but was also evident between muscle layers and in the lamina propria (Fig. 3c, 3rd column). 8- and 12-week-old SHIP$^{-/-}$PI3Kp110δ$^{+/+}$ mice had the largest amount of collagen present, which was reduced by PI3Kp110δ deficiency (Fig. 3c, 4th column).

p110δ activity can be targeted pharmacologically

The ICOS compound, IC87114, is an isoform-specific inhibitor for the p110δ catalytic subunit of PI3K, which does not target other catalytic isoforms.[18] Macrophage colony stimulating factor (MCSF)-derived bone marrow macrophages from SHIP$^{-/-}$ mice were activated with IL-4 and treated with IC87114 or PEG400, as a vehicle control. Untreated SHIP$^{-/-}$ macrophages did not express arg1 (Fig. 4a). IL-4-induced arg1 expression in SHIP$^{-/-}$ macrophages was lower in IC87114-treated macrophages compared to vehicle control (Fig. 4a). Similarly, arginase activity was not present in untreated SHIP$^{-/-}$ macrophages and IL-4 induced arginase activity was lower in IC87114-treated macrophages compared to vehicle control (Fig. 4b).

SHIP$^{-/-}$ mice (8-week-old) were treated with IC87114 daily by oral gavage for 2 weeks. Arginase activity was reduced in ileal tissue cross-sections from mice treated with IC87114 compared to untreated and vehicle-treated control mice (Fig. 4c). Arg1 and Ym1 protein were stained in distal ilea cross-sections from mice. Similar to germline PI3Kp110δ deficiency in SHIP$^{-/-}$ mice, SHIP$^{-/-}$ mice

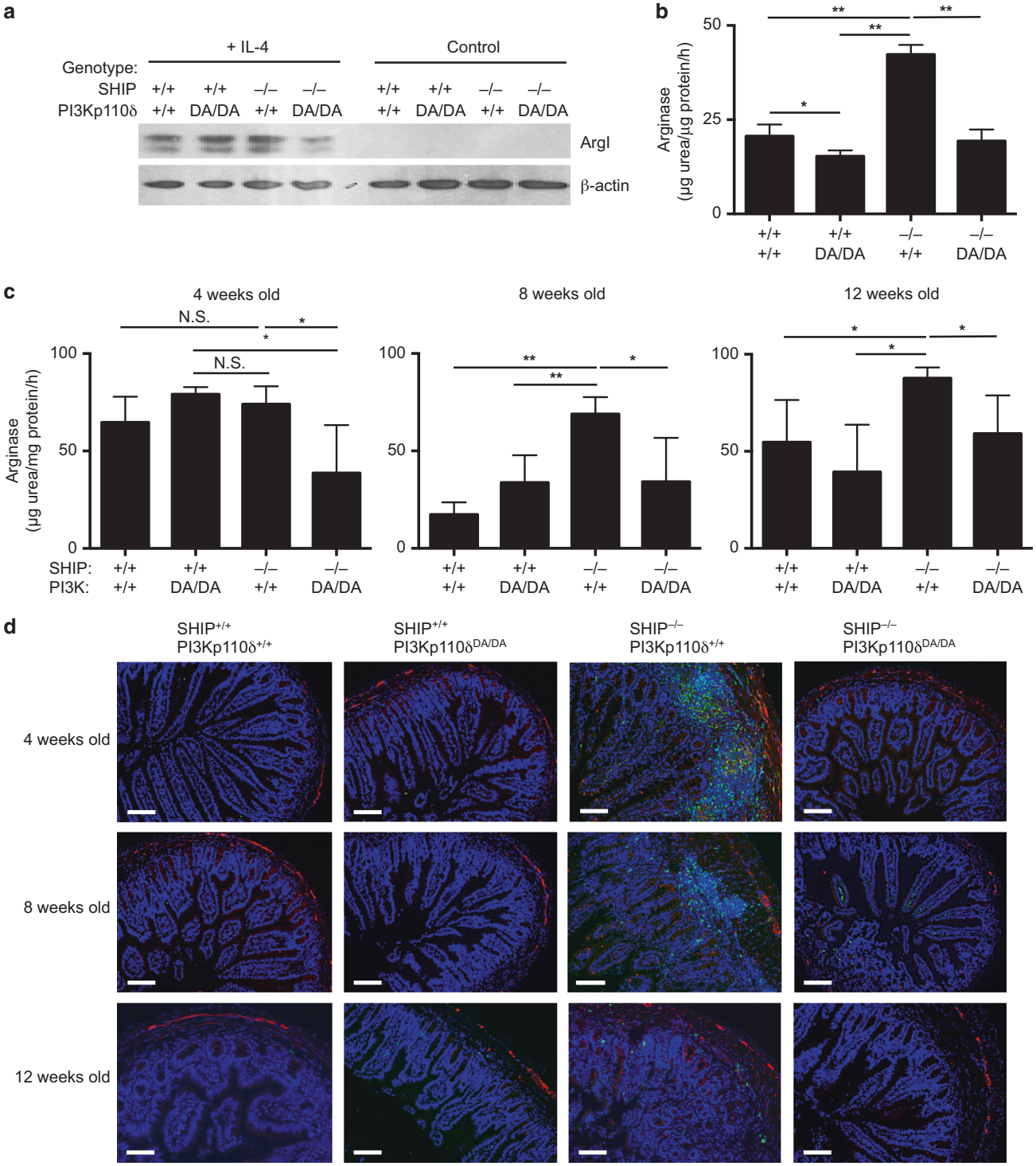

treated with IC87114 had significantly lower numbers of cells expressing argI (red) and Ym1 (green) in the muscle layers and the submucosa of their distal ilea compared to the disease control and vehicle control-treated SHIP$^{-/-}$ mice (Fig. 4d).

Inhibiting p110δ activity reduces gross and histological pathology in SHIP$^{-/-}$ mice

Pathology was compared in 10-week-old SHIP$^{-/-}$ mice treated with IC87114 and PEG400, and to 8-week-old SHIP$^{-/-}$ mice that were untreated. Mice treated with PEG400 (vehicle control) were similar to the untreated SHIP$^{-/-}$ mice (disease control), both of which developed discontinuous patches of muscle thickening and redness in their distal ilea (Fig. 5a). In contrast, SHIP$^{-/-}$ mice that were treated with IC87114 had reduced muscle thickening and redness in their distal ilea (Fig. 5a). Ileal tissue cross-sections were stained by H&E. Disease control and PEG400-treated mice had thick muscle layers accompanied by goblet cell hyperplasia and hypertrophy, crypt-villus hyperplasia, and an abundance of immune cell infiltrates throughout the gut wall (Fig. 5b). SHIP$^{-/-}$ mice treated with IC87114 had reduced immune cell infiltration,

Fig. 1 Genetic deficiency in p110δ activity reduced IL-4-induced arginase I expression in SHIP$^{-/-}$ mice. Mice heterozygous for SHIP expression (SHIP$^{+/-}$) and PI3Kp110δ activity (PI3Kp110δ$^{+/DA}$) were crossed to generate SHIP$^{+/+}$PI3Kp110δ$^{+/+}$, SHIP$^{+/+}$PI3Kp110δ$^{DA/DA}$, SHIP$^{-/-}$PI3Kp110δ$^{+/+}$, and SHIP$^{-/-}$PI3Kp110δ$^{DA/DA}$ mice. **a** MCSF-derived BM macrophages were treated with IL-4 and argI expression was assessed by western blotting using an anti-argI antibody (BD Transduction Laboratories, 19/Arginase I, cat# 610708) and β-actin (Cell Signalling Technologies, 13E5, cat# 4970s) as a loading control. Data are representative of three individual experiments. **b** Arginase activity was measured in IL-4-treated macrophages by measuring the concentration of urea generated by arginase-dependent hydrolysis of L-arginine. Data presented are means ± SD for macrophages from $n = 3$ mice (two male and one female) per genotype assessed in three independent experiments. **c** Arginase activity was also assessed in full-thickness ileal tissue homogenates from mice at 4, 8, and 12 weeks of age. Data presented are means ± SD for $n = 6$ mice (three male and three female) per genotype at each age. In all, ≤1 mouse per genotype was assessed in each independent experiment (>18 independent experiments). For **b**, **c**, $^{*}P < 0.05$, $^{**}P < 0.01$, N.S. = not significantly different using a one-way ANOVA with Bonferroni correction for multiple comparisons. **d** Fixed ileal cross-sections were co-stained with anti-argI (red; BD Biosciences, clone 19, cat #610708), anti-Ym1 (green; StemCell Technologies, cat # 60130), and counterstained with DAPI. Photographs were taken at ×20 magnification; scale bars = 100 μm. Sections are from male mice and are representative of six individual mice (three male and three female) per genotype at each age, harvested in independent experiments

crypt-villus hyperplasia, and muscle thickness compared to both control mice (Fig. 5b).

Inhibiting p110δ activity reduces ileal fibrosis in SHIP$^{-/-}$ mice

Markers of ileal fibrosis, muscle thickness and collagen deposition, were assessed in SHIP$^{-/-}$ mice before and after treatment with IC87114 or vehicle. SHIP$^{-/-}$ mice and vehicle-treated mice had thickened muscle layers, which were reduced by inhibiting p110δ (Fig. 6a). Soluble collagen concentrations were significantly lower in IC87114-treated SHIP$^{-/-}$ mice relative to both 8-week-old SHIP$^{-/-}$ mice and vehicle-treated SHIP$^{-/-}$ mice. In Masson's trichrome-stained sections, control mice (8-week-old SHIP$^{-/-}$) and vehicle-treated mice (PEG400) had high levels of collagen deposition (blue) in the submucosa and muscle layers of their distal ilea, whereas SHIP$^{-/-}$ mice treated with IC87114 had significantly lower amounts of collagen deposition in their distal ilea (Fig. 6c). Together, these results suggest that p110δ inhibition can effectively reverse fibrotic pathology in SHIP$^{-/-}$ mice.

Targeting p110δ activity reduces accumulation of vimentin^{+} mesenchymal cells and IL-4 levels in intestinal tissues, but does not affect TGFβ

Fibroblasts are key drivers of intestinal fibrosis,[19] so we stained tissues with vimentin for mesenchymal cells. SHIP$^{-/-}$PI3Kp110δ$^{+/+}$ mice had more vimentin^{+} cells in their distal ilea than healthy control mice. Increased numbers of vimentin^{+} cells were located within the muscle layers, submucosa, and in the lamina propria (Fig. 7a). SHIP$^{-/-}$PI3Kp110δ$^{DA/DA}$ mice had fewer vimentin^{+} mesenchymal cells in their ilea than their SHIP$^{-/-}$PI3Kp110δ$^{+/+}$ counterparts (Fig. 7a, top). Similarly, SHIP$^{-/-}$ mice that were treated with IC87114 had fewer vimentin^{+} cells in their distal ilea compared to vehicle-treated mice or 8-week-old SHIP$^{-/-}$ mice (Fig. 7a, bottom).

TGFβ was measured in full-thickness ileal homogenates from the mice. Consistent with previous findings, TGFβ concentrations were not elevated in ilea from SHIP-deficient mice[19] and were not altered by genetic deficiency or inhibition of p110δ activity (Fig. 7b). IL-4 concentrations were elevated in the ilea from SHIP$^{-/-}$PI3Kp110δ$^{+/+}$ mice relative to SHIP$^{+/+}$PI3Kp110δ$^{+/+}$ and SHIP$^{+/+}$PI3Kp110δ$^{DA/DA}$ mice, and were reduced in SHIP$^{-/-}$PI3Kp110δ$^{DA/DA}$ mice (Fig. 3c, left). Similarly, SHIP$^{-/-}$ mice treated with the p110δ inhibitor, IC87114, had significantly reduced IL-4 concentrations in their distal ilea compared to the disease control and vehicle control-treated mice (Fig. 3c, right). Taken together, this data reinforces the importance of the IL-4/p110δ signaling pathway in the development of CD-like intestinal fibrosis in the SHIP$^{-/-}$ mouse,[19,21] and suggests that fibrosis develops through a pathway independent of TGFβ in this model.

A newly identified atypical monocyte, referred to as segregated-nucleus-containing atypical monocyte (SatM), up-regulates mRNA encoding the CCAAT/enhancer binding protein B (C/EBPβ), which is required for development of arginase-dependent, but TGFβ-independent, fibrosis during bleomycin-induced lung fibrosis in mice.[23] Thus, we measured *cebpb* mRNA expression in ileal tissue homogenates and colonic mononuclear cells. *Cebpb* mRNA expression was elevated in full-thickness ileal tissue homogenates and further enriched in colonic mononuclear cells from 8-week-old SHIP$^{-/-}$PI3Kp110δ$^{+/+}$ mice and reduced in their SHIP$^{-/-}$PI3Kp110δ$^{DA/DA}$ counterparts (Supplementary Fig. 2a). Similarly, SHIP$^{-/-}$ mice that were treated with IC87114 had reduced *cebpb* mRNA expression in ileal tissue homogenates and colonic mononuclear cells compared to control mice (Supplementary Fig. 2b).

Deficiency in p110δ activity reduces inflammatory pathology in SHIP$^{-/-}$ mice

Together with fibrotic pathology, p110δ deficiency or inhibition appeared to reduce inflammation in SHIP$^{-/-}$ mice (Figs. 2b and 5b). Healthy control mice (SHIP$^{+/+}$PI3Kp110δ$^{+/+}$ and SHIP$^{+/+}$PI3Kp110δ$^{DA/DA}$) at 4 and 8 weeks of age had significantly lower numbers of immune cells in their distal ilea compared to SHIP$^{-/-}$PI3Kp110δ$^{+/+}$ mice, which were reduced in SHIP$^{-/-}$PI3Kp110δ$^{DA/DA}$ mice (Fig. 8a, top). Furthermore, goblet cell numbers (hyperplasia) were elevated in 4- and 8-week-old SHIP$^{-/-}$PI3Kp110δ$^{+/+}$ mice compared to SHIP sufficient controls, and were significantly reduced in SHIP$^{-/-}$PI3Kp110δ$^{DA/DA}$ compared to SHIP$^{-/-}$PI3Kp110δ$^{+/+}$ mice (Fig. 8a, bottom). Pharmacological inhibition of p110δ activity also significantly reduced immune cell infiltrates and goblet cell hyperplasia in SHIP$^{-/-}$ mice (Fig. 8b).

p110δ contributes to increased macrophage IL-1β production in SHIP$^{-/-}$ mice

IL-4-induced arginase activity may reduce inflammation in mice because arginase is an endogenous inhibitor of inflammatory nitric oxide production, so nitric oxide was measured indirectly in full-thickness tissue homogenates from mice using the Griess assay. SHIP deficiency did not correlate with increased nitrite or nitrate levels in tissue homogenates from mice and was not reduced by either genetic or biochemical p110δ deficiency (Supplementary Fig. 1).

IL-1β was measured in full-thickness tissue homogenates from mice because intestinal inflammation in SHIP$^{-/-}$ mice has been attributed to macrophage-derived IL-1β production.[24] SHIP$^{-/-}$PI3Kp110δ$^{+/+}$ mice had significantly higher concentrations of IL-1β in their distal ilea compared to SHIP sufficient controls, which was reduced in SHIP$^{+/+}$PI3Kp110δ$^{DA/DA}$ mice (Fig. 9a, left). IC87114-mediated inhibition of p110δ also reduced ileal IL-1β concentrations in full-thickness tissue homogenates from SHIP$^{-/-}$ mice compared to untreated 8-week-old SHIP$^{-/-}$ mice or PEG400 vehicle-treated control mice (Fig. 9a, right). As an additional control, IL-6 levels were not increased in SHIP-deficient mice and targeting p110δ activity either genetically or biochemically did not reduce IL-6 levels in ileal tissue homogenates (Fig. 9b). Given that macrophages are the source of IL-1β in the inflamed SHIP$^{-/-}$ mouse ileum,[24] macrophages were also quantitated in ileal tissue

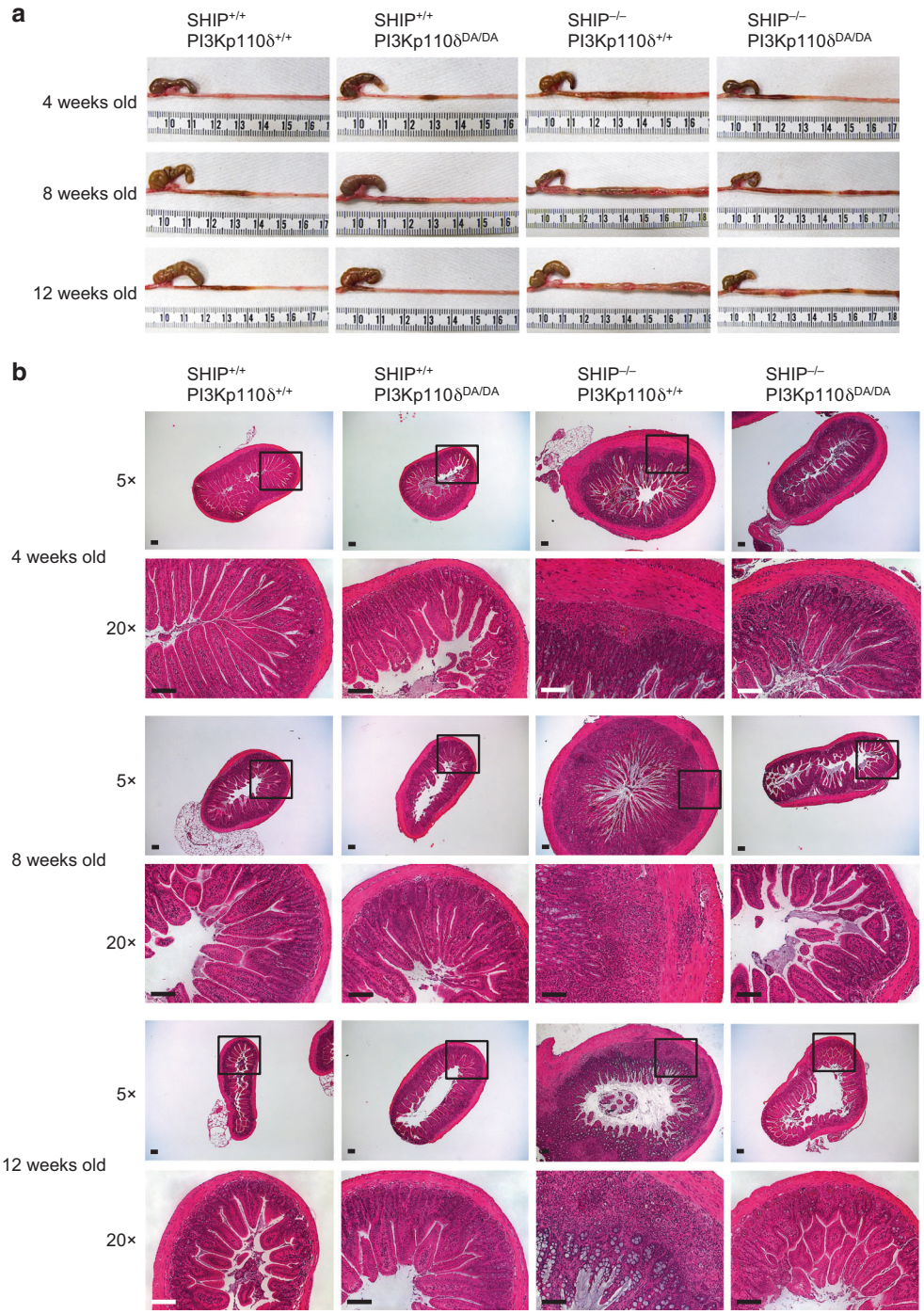

Fig. 2 Deficiency in PI3Kp110δ activity reduced gross pathology and histopathology in SHIP$^{-/-}$ mice. SHIP$^{+/+}$PI3Kp110δ$^{+/+}$, SHIP$^{+/+}$PI3Kp110δ$^{DA/DA}$, SHIP$^{-/-}$PI3Kp110δ$^{+/+}$, and SHIP$^{-/-}$PI3Kp110δ$^{DA/DA}$ mice were euthanized at 4, 8, or 12 weeks of age. **a** Gross anatomy of ceca and distal ilea were photographed. Photographs are male mice and are representative of $n = 6$ mice (three male and three female) per genotype at each age. **b** H&E stained ileal cross sections from male mice were photographed at ×5 and ×20 magnification; scale bars = 100 μm. Sections are representative of $n = 6$ mice (three male and three female) per genotype at each age. Mice were harvested independently and sections were cut and H&E stained in random groups

sections. There were significantly more macrophages in ileal tissues from SHIP$^{-/-}$PI3Kp110δ$^{+/+}$ mice compared to SHIP$^{+/+}$PI3Kp110δ$^{+/+}$ or SHIP$^{+/+}$PI3Kp110δ$^{DA/DA}$ mice and macrophage numbers were significantly reduced in SHIP$^{-/-}$PI3Kp110δ$^{DA/DA}$ mice compared to SHIP$^{-/-}$PI3Kp110δ$^{+/+}$ mice (Fig. 9c, left). Similarly, biochemical inhibition of p110δ activity reduced the number of macrophages in ileal tissues compared to that seen in 8-week-old SHIP$^{-/-}$ mice or vehicle-treated control mice (Fig. 9c, right). Finally, ileal cross-sections from mice were stained with YVAD-FLICA, a fluorescently labeled peptide that binds to the active site of caspase-1, which is required for IL-1β production. In SHIP$^{-/-}$ mice, subepithelial immune cells stained with YVAD-FLICA and staining was reduced in ileal sections from SHIP$^{-/-}$PI3Kp110δ$^{DA/DA}$ mice and in SHIP$^{-/-}$ mice treated with IC87114 (Fig. 9d).

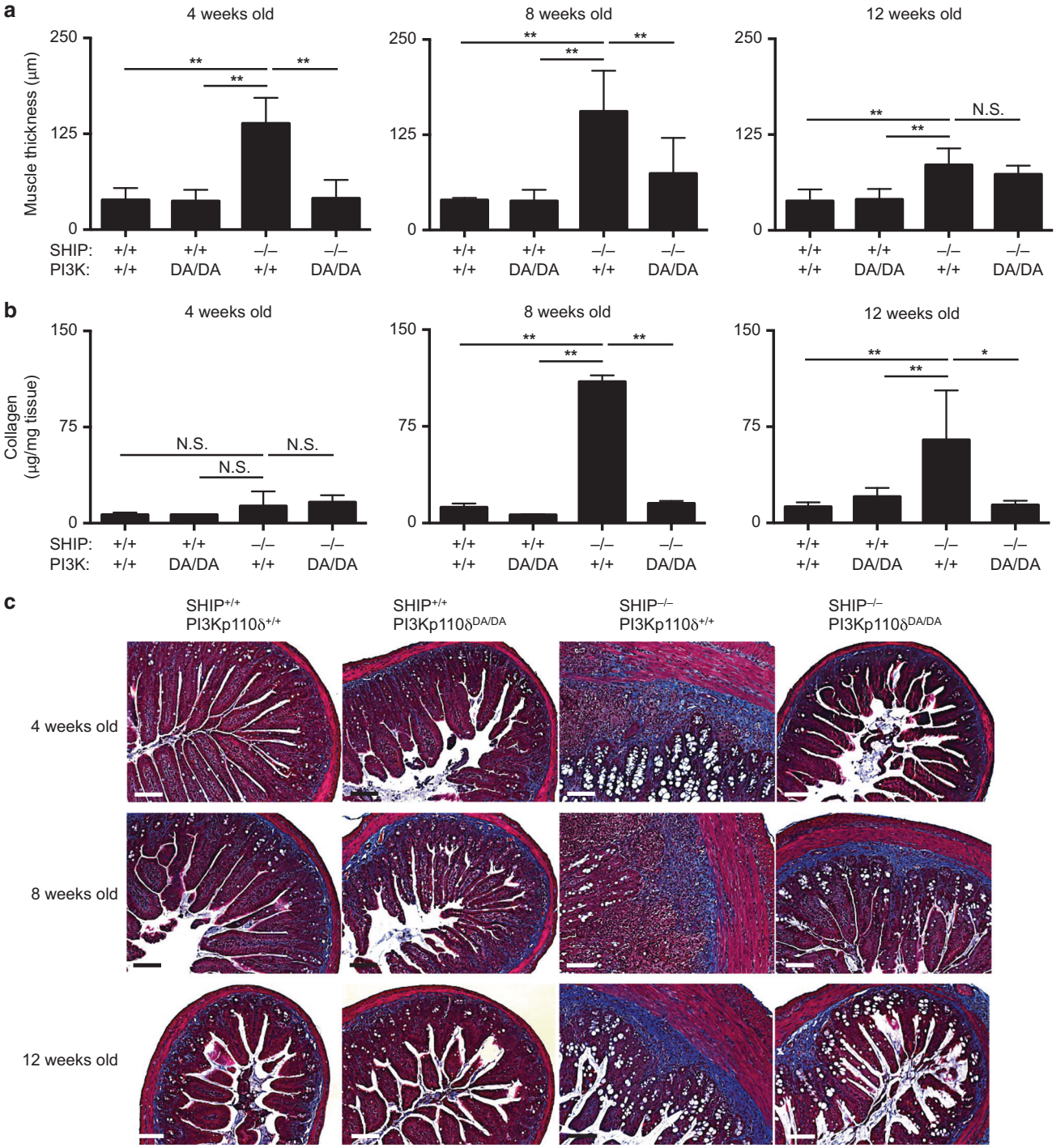

Fig. 3 Deficiency in PI3Kp110δ activity reduced fibrosis in SHIP$^{-/-}$ mice. SHIP$^{+/+}$PI3Kp110δ$^{+/+}$, SHIP$^{+/+}$PI3Kp110δ$^{DA/DA}$, SHIP$^{-/-}$PI3Kp110δ$^{+/+}$, and SHIP$^{-/-}$PI3Kp110δ$^{DA/DA}$ mice were euthanized at 4, 8, and 12 weeks of age. **a** Muscle thickness was measured in H&E stained ileal tissue cross sections from mice. For each mouse, muscle thickness was measured at 6 points on 10 uniform horizontal cross sections separated by ≥50 μm. Data presented are means ± SD for $n = 6$ mice (three male and three female) per genotype at each age. Mice were harvested independently and sections were cut and H&E stained in random groups. **b** Collagen was measured in full-thickness tissue homogenates from mice using the Sircol assay for soluble collagen. Data presented are the means ± SD for $n = 6$ mice (three male and three female) per genotype at each age. In all, ≤1 mouse per genotype was assessed in each independent experiment (>18 independent experiments). For **a**, **b** $^{*}P < 0.05$, $^{**}P < 0.01$, N.S. = not significantly different using a one-way ANOVA with Bonferroni correction for multiple comparisons. **c** Fixed ileal cross sections were stained with Masson's trichrome for fibrosis; collagen is stained blue. Photographs of sections from male mice were taken at ×20 magnification; scale bars = 100 μm. Sections are representative of six mice (three male and three female) per genotype at each age. Mice were harvested independently and sections were cut and stained in random groups

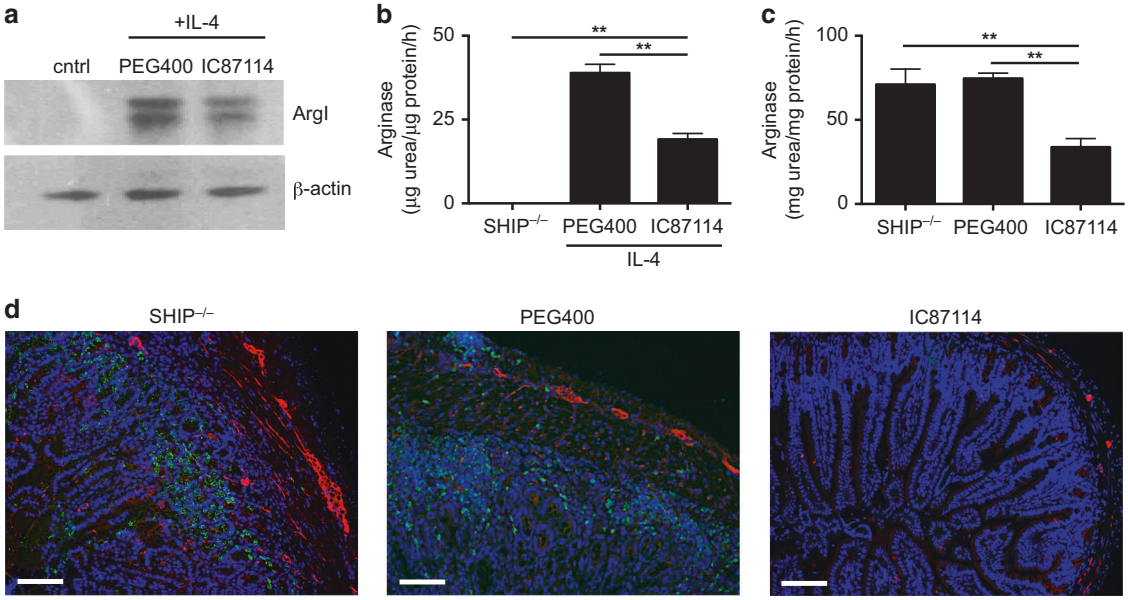

Fig. 4 Inhibiting p110δ activity reduced IL-4-induced arginase I expression in SHIP$^{-/-}$ macrophages and mice. The PI3Kp110δ isoform-specific inhibitor, IC87144, was used to inhibit p110δ activity in IL-4-treated SHIP$^{-/-}$ macrophages or in SHIP$^{-/-}$ mice and arginase expression and activity were assessed. **a** MCSF-derived SHIP$^{-/-}$ BM macrophages were treated with IL-4 in in the presence of IC87114, or PEG400, as a vehicle control. ArgI expression was assessed by western blotting using an anti-argI antibody (BD Transduction Laboratories, 19/Arginase I, cat# 610708) and β-actin (Cell Signalling Technologies, mAb 13E5, cat# 4970s) as a loading control. Data shown are from macrophages harvested from a female mouse and are representative of three independent experiments performed on macrophages from one male and two female SHIP$^{-/-}$ mice. **b** Arginase activity was measured in IL-4-treated macrophages by measuring the concentration of urea generated by arginase-dependent hydrolysis of L-arginine. Data presented are means ± SD for macrophages from $n = 3$ mice (one male and two female) per group assessed in three independent experiments. **c** SHIP$^{-/-}$ mice were untreated or treated with IC87114, or PEG400 (vehicle control), daily by oral gavage for 2 weeks from 8–10 weeks of age. Arginase activity was assessed in full-thickness ileal tissue homogenates from mice. Data presented are means ± SD for $n =$ six mice (three male and three female) per group assessed in six independent experiments. For **b**, **c** $^{**}P < 0.01$ using a one-way ANOVA with Bonferroni correction for multiple comparisons. **d** Fixed ileal cross-sections were co-stained with anti-argI (red; BD Biosciences, clone 19, cat #610708), anti-Ym1 (green; StemCell Technologies, cat # 60130), and counterstained with DAPI. Photographs were taken at ×20 magnification; scale bars = 100 μm. Sections are from male mice and are representative of six individual mice (three male and three female) per group

DISCUSSION

We provide genetic and biochemical evidence that demonstrate a critical role for the PI3Kp110δ catalytic subunit of Class I PI3K in driving intestinal fibrosis in SHIP$^{-/-}$ mice.

PI3Kp110δ activity must be tightly regulated as both loss- and gain-of-function mutations can cause immune-mediated disease.[25] Mice deficient in PI3Kp110δ have been reported to develop spontaneous colonic inflammation[17]; though mice in our colony do not develop spontaneous colitis,[18] we have found that they are more susceptible to DSS-induced colitis than their wild type littermates due to defects in IL-4-mediated activation of PI3Kp110δ deficient macrophages.[18] PI3Kp110δ and its downstream target, Akt, are activated in response to IL-4 in macrophages as well as NK, B, and T cells.[16,21,26] In macrophages, IL-4 induces PI3Kp110δ to drive transcription of argI, which is protective against intestinal inflammation, but contributes to intestinal fibrosis.[19,27] In SHIP$^{-/-}$ mice, PI3Kp110δ deficiency or inhibition may compromise development or survival of fibrosis-inducing cells, as suggested by a loss of argI-expressing cells in ileal tissue sections. Our data are consistent with a model in which loss of SHIP leads to increased and/or prolonged PI3Kp110δ activity mimicking a gain-of-function mutation in PI3Kp110δ.

TGFβ has been found in high amounts in the inflamed gut of CD patients and has been implicated in executing the steps that initiate and perpetuate fibrosis.[28] TGFβ can contribute to intestinal fibrosis directly by stimulating fibroblasts to produce interstitial fibrillar collagen, and indirectly by up-regulating PDGF receptors on fibroblasts increasing fibroblast survival, proliferation, and migration to sites of injury.[28] TGFβ is not up-regulated in the distal ileum of SHIP$^{-/-}$ mice[19] and we found that TGFβ concentrations did not correlate with reduced fibrosis when PI3Kp110δ activity was genetically ablated or pharmacologically inhibited in SHIP$^{-/-}$ mice. Despite that, vimentin^{+} mesenchymal cell (e.g. fibroblast) numbers were significantly reduced in the absence of PI3Kp110δ activity, as were collagen accumulation and soluble collagen levels. Arginase-dependent, but TGFβ-independent fibrosis has been attributed to increased *cebpb* gene expression in 'SatM' mononuclear cells in the mouse model of bleomycin-induced lung fibrosis.[23] Consistent with that, *cebpb* gene expression is increased in ileal tissue homogenates and ileal mononuclear cells from SHIP$^{-/-}$ mice and reduced by genetic ablation or pharmacological inhibition of PI3Kp110δ activity. This suggests that this atypical monocyte population may contribute to ileal fibrosis in SHIP-deficient mice and be regulated by PI3Kp110δ activity. Moreover, PI3Kp110δ is upstream of C/EBPβ activation. IL-4-mediated PI3Kp110δ activation leads to phosphorylation/inactivation of GSK3β and this positively regulates CREB, which in turn activates C/EBPβ-driven transcription.[21] The argI promoter has C/EBPβ binding sites and our laboratory has speculated previously that STAT6-mediated transcription cooperates with the transcription factor C/EBPβ to drive argI gene expression downstream of IL-4.[21] PI3Kp110δ deficiency or inhibition may reduce fibrosis independent of TGFβ, as mice lacking PI3Kp110δ activity have lower levels of C/EBPβ expressing mononuclear cells (the SatM population) and reduced C/EBPβ-induced transcription compared to SHIP$^{-/-}$ disease control mice.

In addition, fibrosis is associated with a T helper type 2 cytokine profile, specifically high levels of IL-4 and IL-13.[29] IL-4 and IL-13 are up-regulated in the inflamed ilea of SHIP$^{-/-}$ mice and may be sufficient to drive fibrosis.[19,30] In a second mouse model of ileal

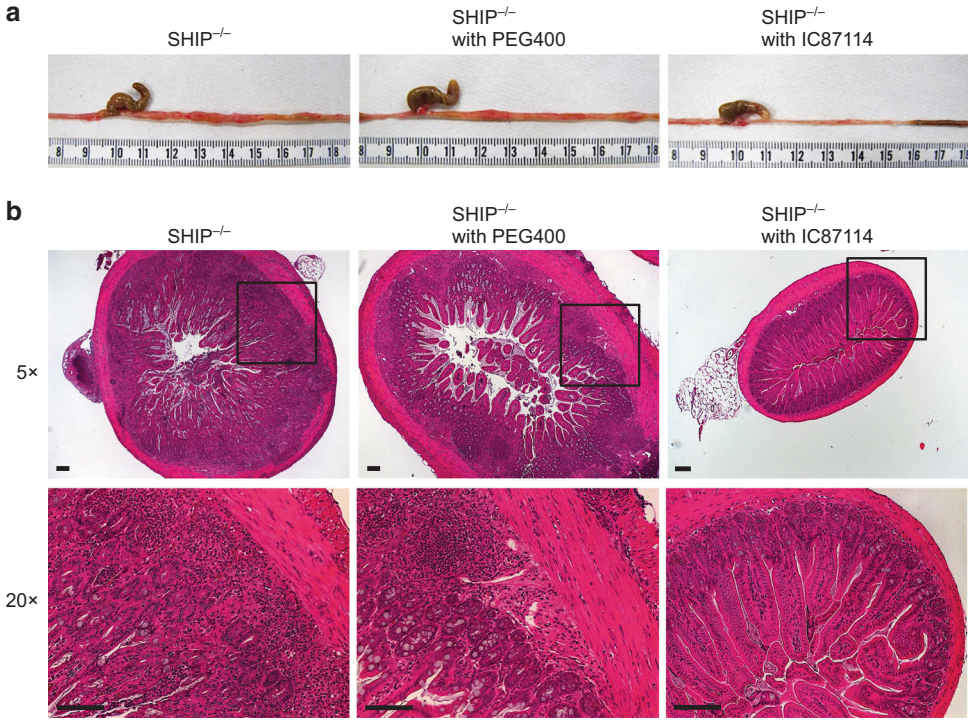

Fig. 5 Inhibiting p110δ activity reduced gross pathology and histopathology in SHIP$^{-/-}$ mice. SHIP$^{-/-}$ mice were treated with the p110δ isoform-specific inhibitor, IC87144, daily by oral gavage for 2 weeks, from 8 to 10 weeks of age. IC87114-treated mice were compared to PEG400 vehicle-treated control mice and 8-week-old, untreated SHIP$^{-/-}$ mice. **a** Gross anatomy of ceca and distal ilea were photographed. Photographs are from female mice and are representative of $n = 6$ mice (three male and three female) per group. **b** H&E stained ileal cross sections from mice were photographed at ×5 and ×20 magnification; scale bars = 100 μm. Sections are from female mice and are representative of $n = 6$ mice (three male and three female) per group. Experiments were performed using three sex-matched SHIP$^{-/-}$ mice per experiment in six independent experiments

inflammation and fibrosis, the SAMP1/YitFc mice, the chronic inflammatory stage of disease is characterized by a mixed type 1/type 2 immune response with high concentrations of IL-4 and IL-13, and an anti-IL-4 blocking antibody reduced intestinal pathology in SAMP1/YitFc mice.[31–33] IL-4 and IL-13 signal through the IL-4 receptor (type I or II, respectively) activating the AKT/mTOR signal transduction pathway leading to the proliferation and activation of fibroblasts, which deposit extracellular matrix into the surrounding connective tissue.[34] Macrophages from SHIP$^{-/-}$ mice are hyper-responsive.[15] High basal IL-4 expression,[35] together with increased responses to IL-4,[21] causes IL-4 activation of in vivo differentiated SHIP$^{-/-}$ macrophages.[36] In addition, argI is expressed by neutrophils in the inflamed ilea of SHIP$^{-/-}$ mice[19] so argI expression by macrophages and neutrophils may both contribute to the intestinal fibrosis in the SHIP$^{-/-}$ mouse ileum.[19] Arginase activity leads to the production of polyamines, spermine and spermidine, which promote fibroblast growth and production of interstitial fibrillar collagen, and the production of L-proline, an essential amino acid in the collagen triple-helix structure.[37,38] Taken together, evidence suggests that IL-4/IL-13 signaling through PI3Kp110δ may activate fibroblasts and induce fibrosis, circumventing the requirement for TGFβ in SHIP deficiency.

Genetic or pharmacological inhibition of PI3Kp110δ also reduced inflammation in SHIP$^{-/-}$ mice, which was unexpected, as the following lines of evidence suggested that targeting PI3Kp110δ would not affect, or could exacerbate, intestinal inflammation. Macrophage-derived IL-1β drives inflammation in SHIP$^{-/-}$ mice but it is up-regulated by PI3Kp110α-dependent transcription of *Il1b*, and independent of PI3Kp110δ.[24] In addition, PI3Kp110δ-induced arginase activity is expected to be anti-inflammatory as arginase can compete with inducible nitric oxide synthase for their common substrate, L-arginine, thereby limiting production of inflammatory nitric oxide.[18] PI3Kp110δ has also been implicated in the generation and function of anti-inflammatory myeloid-derived suppressor cells and Tregs.[39] Finally, macrophages deficient in PI3Kp110δ release IL-1β, which is dependent on MEFV (pyrin) but independent of the NLRP3, AIM1, or AIM2 inflammasomes,[40] suggesting that targeting PI3Kp110δ might be hypothesized to increase IL-1β-driven intestinal inflammation in SHIP$^{-/-}$ mice, contrary to what we found. It is well-accepted that chronic inflammation can initiate fibrosis[7] and more recently, fibrosis has been recognized as a self-perpetuating process driven by independent mechanisms,[41] but it is possible that this does not occur in the absence of inflammation.

Alternatively, PI3Kp110δ may contribute to inflammation in SHIP$^{-/-}$ mice directly. Indeed, loss of PI3Kp110δ activity ameliorated both spontaneous lung and intestinal inflammation in the SHIP$^{-/-}$ mice. SHIP$^{-/-}$ mouse lung inflammation may be driven by type II cytokines, which are also elevated and may contribute to intestinal inflammation in SHIP$^{-/-}$ mice. There is a striking paucity of T cells, including Tregs, in the SHIP$^{-/-}$ ileum[20] and a comparable reduction in SHIP$^{-/-}$ mouse lung and intestinal inflammation occurs when mice are treated with a Caspase 8 inhibitor, which has been attributed to improved survival of T cells.[42] In T cells from people with gain-of-function mutations in PI3Kp110δ, inhibition of PI3Kp110δ blocks expression of effector cytokines, IL-4 and IL-17, which may explain why IL-4 concentrations were reduced in SHIP$^{-/-}$ mice when PI3Kp110δ activity was targeted.[43] PI3Kp110δ has also been shown to play a role in the chemoattractant-mediated migration of peripheral neutrophils and macrophages to sites of injury[39] and argI-expressing neutrophils and macrophages comprise the vast majority of infiltrating immune cells in the SHIP$^{-/-}$ mouse ileum.[19] In

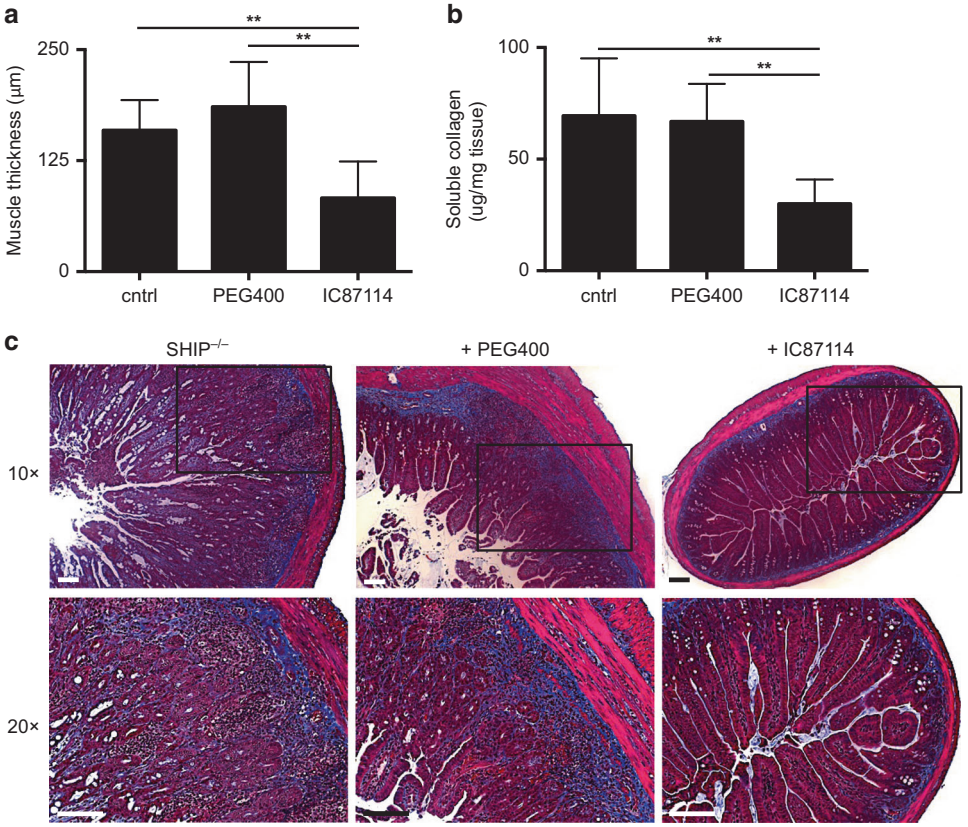

Fig. 6 Inhibiting p110δ activity reduced fibrosis in SHIP$^{-/-}$ mice. SHIP$^{-/-}$ mice were treated with the p110δ isoform-specific inhibitor, IC87144, daily by oral gavage for 2 weeks, from 8 to 10 weeks of age. IC87114-treated mice were compared to PEG400 vehicle-treated control mice and 8-week-old, untreated SHIP$^{-/-}$ mice. **a** Muscle thickness was measured in H&E stained ileal tissue cross sections from mice. For each mouse, muscle thickness was measured at 6 points on 10 uniform horizontal cross sections separated by ≥50 μm. Data presented are means ± SD for $n = 6$ mice (three male and three female) per group. **b**) Collagen was measured in full-thickness tissue homogenates from mice using the Sircol assay for soluble collagen. Data presented are the means ± SD for $n = 6$ mice (three male and three female) per group. For **a**, **b**, $^{**}P < 0.01$, N.S. = not significantly different using a one-way ANOVA with Bonferroni correction for multiple comparisons. **c** Fixed ileal cross sections were stained with Masson's trichrome for fibrosis; collagen is stained blue. Photographs were taken of sections from female mice at ×10 and ×20 magnification; scale bars = 100μm. Sections are representative of six mice (three male and three female) per group. Experiments were performed using three sex-matched SHIP$^{-/-}$ mice per experiment in six independent experiments

addition, PI3Kp110δ is required for ROS production by human neutrophils.[44] Thus, it is possible that the PI3Kp110δ/SHIP signaling axis contributes to both inflammation and fibrosis independently or cooperatively, with each process influencing the other.

An additional source of cross-talk between inflammatory and fibrotic pathways is the cytokine, IL-1β. IL-1β is not only a key pro-inflammatory cytokine, but also activates fibroblasts, thereby contributing to fibrotic pathology.[24,45] In the SHIP$^{-/-}$ mouse, anakinra treatment reduced not only inflammation but also reduced arginase levels, the number of mesenchymal cells, and collagen deposition in the distal ileum of SHIP$^{-/-}$ mice.[24] This is likely a consequence of reducing inflammation, but targeting IL-1 signaling may also have direct effects on IL-1β-mediated activation of fibroblasts that produce collagen. Moreover, SHIP$^{-/-}$ mice, which are also deficient in PI3Kp110δ activity, have reduced IL-1β production compared to the inflamed SHIP$^{-/-}$ control mice, which may contribute directly to both decreased inflammation and fibrosis.

As little as a decade ago, intestinal fibrosis was considered an irreversible consequence of long-term inflammation in people with IBD, particularly those who did not respond to anti-inflammatory therapy.[41] Approximately 20% of people with CD overall, and 30% of people with CD who are referred to tertiary care centers, develop fibrostenotic strictures within 20 years of diagnoses.[46] Moreover, these numbers are based on the Montreal Vienna classification system and likely underestimate the incidence of fibrotic disease.[41] Surgery can remove acute obstructions but fibrosis can recur leading to repetitive stricture formation and obstruction.[47] Anti-fibrotic strategies have been successfully used and can induce regression of fibrosis in other organs including skin, kidney, and liver.[48] Anti-fibrotic treatment may be effective in the gut as well; after strictureplasty, the overall recurrence rate of jejunoileal strictures was only 39% and ileocolonic stricture was only 36%, suggesting that interventions can positively affect the course of disease.[49] Rogler and Hausmann[50] posited that new animal models for intestinal fibrosis may provide insight into mechanisms of disease and identify specific therapies for fibrosis in people with CD.[50] Using the SHIP$^{-/-}$ mouse, we have found that targeting PI3Kp110δ activity can reduce CD-like intestinal fibrosis. A new drug targeting PI3Kp110δ activity, idelalisib, has recently been developed and licensed for use in the United States and European Union for the treatment of B cell neoplasms.[51] We, and others, have reported that a subset of people with CD have very low SHIP activity.[24,52] Kerr's group has gone on to show that SHIP deficiency in CD is associated with increased surgeries associated with fibrotic complications.[53] Thus, people with CD and low SHIP activity may be at increased risk of developing fibrosis, which may be amenable

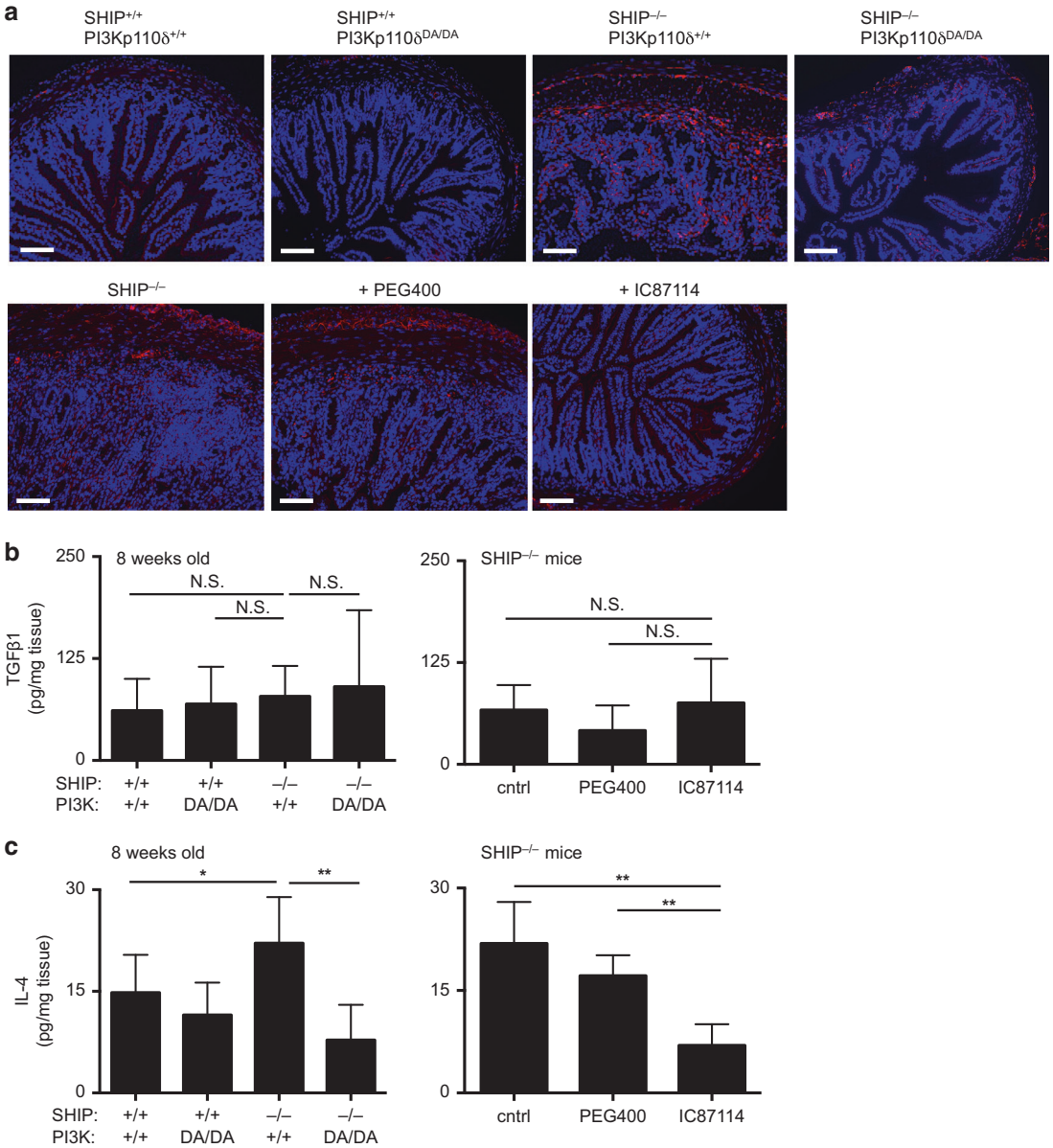

Fig. 7 Loss of p110δ activity reduced vimentin^{+} mesenchymal cells and IL-4, but not TGFβ levels in the distal ileum of SHIP$^{-/-}$ mice. **a** Vimentin staining of ileal tissue cross sections from 8-week-old SHIP$^{+/+}$PI3Kp110δ$^{+/+}$, SHIP$^{+/+}$PI3Kp110δ$^{DA/DA}$, SHIP$^{-/-}$PI3Kp110δ$^{+/+}$, and SHIP$^{-/-}$PI3Kp110δ$^{DA/DA}$ mice (top); and untreated SHIP$^{-/-}$ mice or SHIP$^{-/-}$ mice treated with the p110δ inhibitor, IC87114, or vehicle control, PEG400 (bottom). Anti-vimentin antibody was from BD Pharmingen (clone RV202, cat #550513). Photographs were taken at ×20 magnification; scale bars = 100 μm. Sections are representative of six individual mice per group (three male and three female). Mice from different genotypes were harvested independently and male mouse sections are shown; sex-matched mice from inhibition experiments were assessed in six independent experiments and sections from male mice are shown. TGFβ (**b**) and IL-4 (**c**) were measured in full-thickness ileal tissue homogenates from 8-week-old SHIP$^{+/+}$PI3Kp110δ$^{+/+}$, SHIP$^{+/+}$PI3Kp110δ$^{DA/DA}$, SHIP$^{-/-}$PI3Kp110δ$^{+/+}$, and SHIP$^{-/-}$PI3Kp110δ$^{DA/DA}$ mice (left) and untreated SHIP$^{-/-}$ mice and SHIP$^{-/-}$ mice treated with the p110δ inhibitor, IC87114, or vehicle control, PEG400 (right). Data presented are means ± SD for $n = 8$ mice (four male and four female) per group. Mice from different genotypes were harvested independently (≤1 mouse per genotype harvested in groups of mice) and sex-matched mice from inhibition experiments were assessed in eight independent experiments. *$P < 0.05$, **$P < 0.01$, N.S. = not significantly different using a one-way ANOVA with Bonferroni correction for multiple comparisons

to treatment by targeting PI3Kp110δ. Though PI3Kp110δ inhibition is not predicted to block the inflammation that drives fibrosis in people with CD, it could be used together with biologics as an adjuvant therapy to reduce fibrotic complications. Inhibition of PI3Kp110δ activity with idelalisib or a similar drug may provide a first-in-class therapy to treat CD-associated fibrosis in people with low SHIP activity that can be rapidly translated into clinical application.

METHODS

Mice

Mice homozygous for SHIP deficiency (*Inpp5d*$^{-/-}$) on a mixed C57BL/6 × 129Sv background (F2 generation) were used for inhibitor experiments. SHIP$^{-/-}$ mice were also crossed with mice deficient in PI3Kp110δ activity (PI3Kp110δ$^{D910A/D910A}$; PI3Kp110δ$^{DA/DA}$), which were obtained from the Ludwig Cancer Research Institute (C57BL/6 background).[54] Crossing SHIP$^{-/-}$ and PI3Kp110δ$^{DA/DA}$

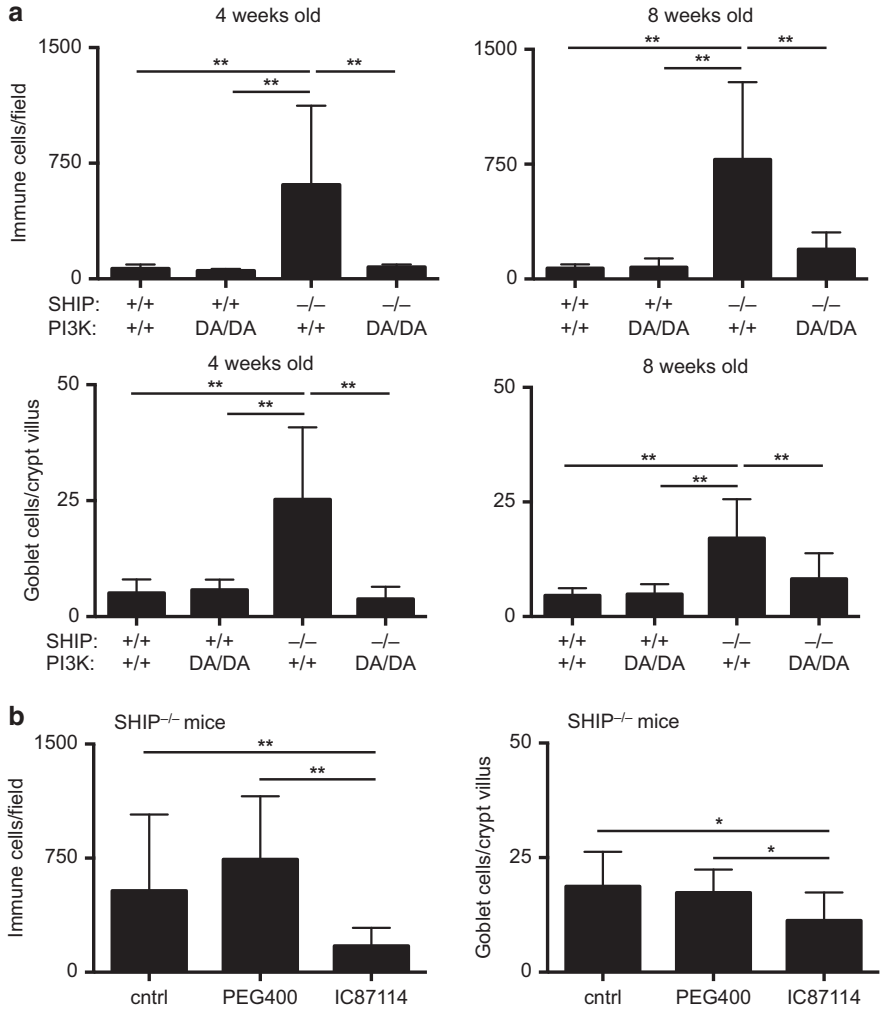

Fig. 8 Loss of p110δ activity reduced histological measures of inflammation in the SHIP$^{-/-}$ mice ilea. **a** Immune cell infiltrates (top) and goblet cells per crypt villus (bottom) were counted in H&E-stained cross sections from 8-week-old SHIP$^{+/+}$PI3Kp110δ$^{+/+}$, SHIP$^{+/+}$PI3Kp110δ$^{DA/DA}$, SHIP$^{-/-}$PI3Kp110δ$^{+/+}$, and SHIP$^{-/-}$PI3Kp110δ$^{DA/DA}$ mice. **b** Immune cell infiltrates (left) and goblet cells per crypt villus (right) were counted in H&E-stained cross sections from 8-week-old SHIP$^{-/-}$ mice and SHIP$^{-/-}$ mice treated with the p110δ inhibitor, IC87114, or vehicle control, PEG400. For each mouse, quantitation was performed on six photographs per section for six uniform horizontal cross sections separated by ≥50 μm. Data presented are means ± SD for $n = 6$ mice (three male and three female) per group. Mice from different genotypes were harvested independently (≤1 mouse per genotype harvested in groups of mice) and sex-matched mice from inhibition experiments were assessed in six independent experiments. *$P < 0.05$, **$P < 0.01$, N.S. = not significantly different using a one-way ANOVA with Bonferroni correction for multiple comparisons

mice generated mice heterozygous for SHIP (SHIP$^{+/-}$) and PI3Kp110δ (PI3Kp110δ$^{+/D910A}$). Subsequent matings were made to generate: SHIP$^{+/+}$PI3Kp110δ$^{+/+}$, SHIP$^{+/+}$PI3KP110δ$^{DA/DA}$, SHIP$^{-/-}$PI3Kp110δ$^{+/+}$, and SHIP$^{-/-}$PI3KP110δ$^{DA/DA}$ mice that were used for experiments (F3 generation). Mice were assessed at 4, 8, 10, or 12 weeks of age. Equal numbers of male and female mice of each genotype were used for analyses. Mice were harvested independently and only one mouse per genotype was selected from any litter. Mice were housed under specific pathogen-free conditions in sterilized filter-top cages and received autoclaved food and water *ad libitum* at the Animal Care Facility at the BC Children's Hospital Research Institute (Vancouver, BC, Canada). All of the animal protocols used were approved by the institutional Animal Care Committee and in accordance with Canadian Council on Animal Care guidelines (Protocol A09-0027 and A09-0032).

Oral gavage

SHIP$^{-/-}$ mice (8-week-old) were given 50 mg/kg IC87114 dissolved in 120–150 μl PEG400 (Hampton Research, Aliso Viejo, CA) or an equal volume of PEG400 (vehicle control) once daily by oral gavage. After 14 days, mice were euthanized, and their distal ilea were removed for analyses. Groups of three sex-matched mice (no treatment, vehicle, or IC87114 treatment) were used in independent experiments for each analysis.

Macrophage derivation and western blotting

Bone marrow macrophages were derived from bone marrow aspirates of femura and tibiae from mice as described previously.[27] 10-day-old macrophages were treated ±10 ng/mL recombinant IL-4 (StemCell Technologies, Vancouver, British Columbia, Canada) for 3 days to induce argI expression.

Whole cell lysates were prepared for SDS-PAGE by lysing in 1 × Laemmli's digestion mix, sheering DNA using a 26 gauge needle and boiling for 1 min. Lysates were separated on a 12% polyacrylamide gel and western blotting was performed. Antibodies used for western blot analyses were anti-argI (19/Arginase I, cat # 610708, BD Transduction Laboratories, Mississauga, ON, Canada) and anti-β-actin (13E5, cat# 4970s, Cell Signalling Technologies).

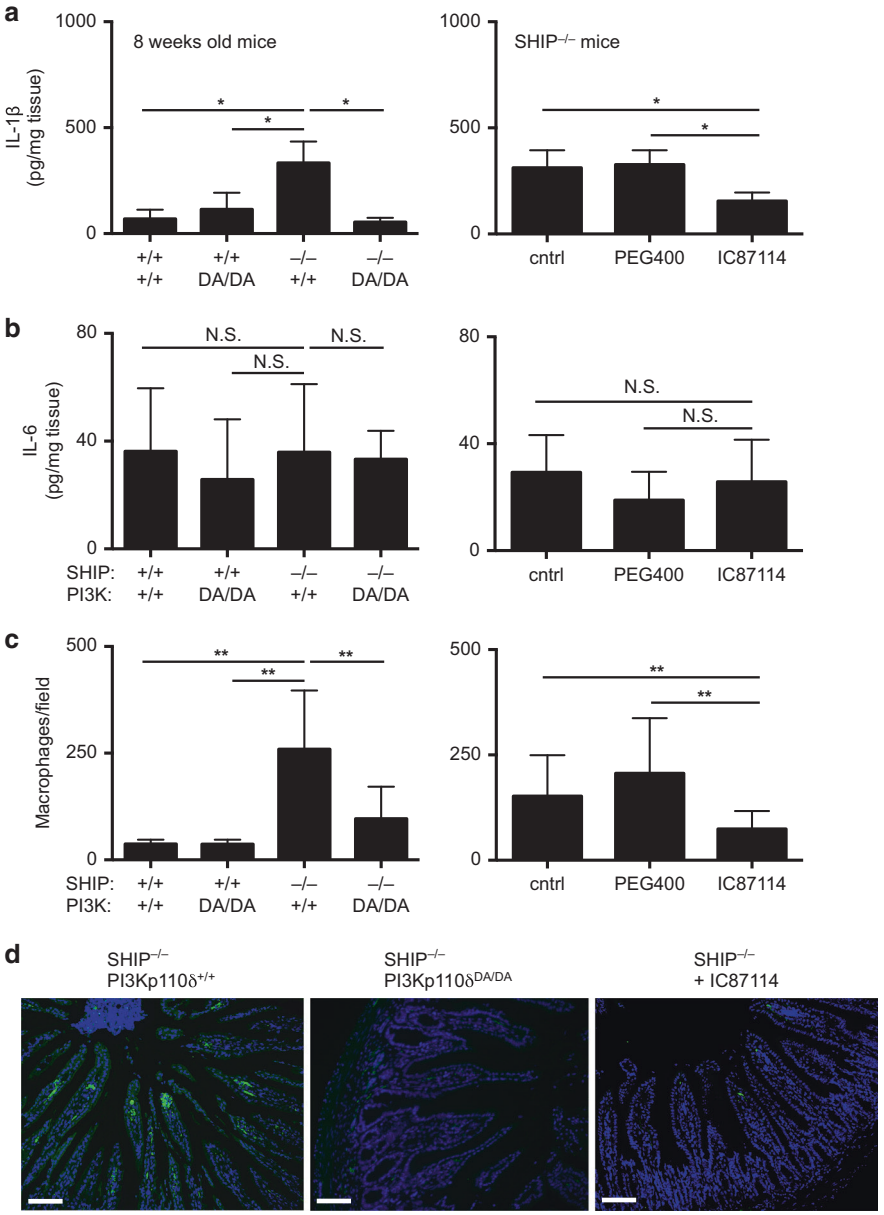

Fig. 9 Loss of p110δ activity reduced IL-1β concentrations and macrophage numbers in the SHIP$^{-/-}$ mice ilea. **a** IL-1β and **b** IL-6 were measured in full-thickness ileal tissue homogenates from 8-week-old SHIP$^{+/+}$PI3Kp110δ$^{+/+}$, SHIP$^{+/+}$PI3Kp110δ$^{DA/DA}$, SHIP$^{-/-}$PI3Kp110δ$^{+/+}$, and SHIP$^{-/-}$PI3Kp110δ$^{DA/DA}$ mice (left) and 8-week-old SHIP$^{-/-}$ mice and SHIP$^{-/-}$ mice treated with the p110δ inhibitor, IC87114, or vehicle control, PEG400 (right). **c** Macrophages were counted in F4/80-stained cross sections from 8-week-old SHIP$^{+/+}$PI3Kp110δ$^{+/+}$, SHIP$^{+/+}$PI3Kp110δ$^{DA/DA}$, SHIP$^{-/-}$PI3Kp110δ$^{+/+}$, and SHIP$^{-/-}$PI3Kp110δ$^{DA/DA}$ mice (left) and 8-week-old SHIP$^{-/-}$ mice and SHIP$^{-/-}$ mice treated with the p110δ inhibitor, IC87114, or vehicle control, PEG400 (right). For each mouse, quantitation was performed on six photographs per section, taken at ×40 magnification, for six uniform horizontal cross sections separated by ≥50 μm. For **a**–**c** data presented are means ± SD for $n = 6$ mice (three male and three female) per group. Mice from different genotypes were harvested independently (≤1 mouse per genotype harvested in groups of mice) and sex-matched mice from inhibition experiments were assessed in six independent experiments. *$P < 0.05$, **$P < 0.01$, N.S. = not significantly different using a one-way ANOVA with Bonferroni correction for multiple comparisons. **d** Fixed ileal cross-sections from SHIP$^{-/-}$PI3Kp110δ$^{+/+}$ mice, and SHIP$^{-/-}$PI3Kp110δ$^{DA/DA}$ mice, and SHIP$^{-/-}$PI3Kp110δ$^{+/+}$ mice treated with IC87114 were stained with YVAD-FLICA (green), and counterstained with DAPI. Photographs were taken at ×20 magnification; scale bars = 100 μm. Sections from male mice are shown and are representative of six individual mice (three male and three female) per group, which were harvested independently

Arginase assay

Fresh tissue samples were collected and homogenized in 1 mL lysis buffer (0.1% Triton X-100, 25 mM Tris pH 8, aprotinin (40 μg/mL), leupeptin (8 μg/mL), PMSF (100 μM)) using a Polytron MR2100 homogenizer. Homogenates were clarified by centrifugation at 16,000 × *g* for 10 min at 4 °C. Arginase activity was determined indirectly by measuring the concentration of urea generated by the arginase-dependent hydrolysis of L-arginine, as previously described.[21]

Immunofluorsecence staining

For immunofluorescent detection of murine argI, Ym1, and vimentin; slide-mounted, 5 μm sections of formalin-fixed, paraffin-embedded tissues were deparaffinized and rehydrated.

Heat-induced epitope retrieval was performed by immersing the slides in 1 mM Ethylenediaminetetraacetic acid (EDTA), pH 8.0, at 95 °C for 20 min and allowing slides to cool to room temperature. All slides were rinsed in Tris-buffered saline with 0.1% Tween-20. Endogenous avidin and biotin were blocked with an avidin-biotin blocking kit, according to manufacturer's instructions (Vector Laboratories, Burlingame, CA, USA). Primary antibodies, including mouse anti-argI (clone 19, cat# 610708, BD Biosciences, Mississauga, Canada), rabbit anti-Ym1 (cat# 60130 StemCell Technologies), mouse anti-vimentin (Vim 3B4, cat # CBL202, MilliporeSigma, Oakville, ON, Canada), anti-SHIP (M-14, cat# sc-1894, Santa Cruz Biotechnology, Mississauga, Ontario, Canada), and anti-p110δ (A-8, cat# sc55589, Santa Cruz Biotechnology) were used. Blocking buffers, secondary Alexa conjugated IgG antibodies (Molecular Probes/Invitrogen, Eugene, OR), and avidin-biotin-HRP were prepared and used from rabbit IgG, or mouse IgG detection kits, according to the manufacturer's instructions (Vector Laboratories). Sections were mounted in Vectashield mounting medium with DAPI (Vector Laboratories). Negative controls, an irrelevant isotype control and no primary antibody, were performed for all staining. Images were acquired and analyzed using a Zeiss Axiovert 200 microscope, a Zeiss AxioCam HR camera, and the Zeiss AxioVision 4.0 software imaging system.

Histological analyses

Mice were euthanized and distal ilea were removed, cleared of contents, and fixed in PBS-buffered 10% formalin. Lungs were removed, filled with, and suspended in PBS-buffered 10% formalin for fixation. Tissue sections were embedded in paraffin, and 5 µm cross-sections were stained with H&E or Masson's trichrome stain, according to manufacturers' instructions (Sigma-Aldrich).

Quantitation of histological measures of pathology was performed on uniform horizontal cross-sections by two trained readers blinded to experimental condition. The thickness of the muscularis externa from the serosa to the muscularis mucosa was measured at 6 points in 10 cross sections separated by >50 µm. To count immune cell infiltrates, six representative fields of H&E-stained cross sections were obtained from each section at ×40 magnification and 6 sections separated by >50 µm were counted for each mouse. Immune cell infiltrates were counted according to nuclear morphological features in the circular muscularis externa and submucosa. Goblet cells per crypt-villus were determined by counting goblet cells from the base of crypts to the villus tip averaging >10 crypt-villus per section in 10 cross-sections separated by >50 µm for each mouse.

Sircol assay

Sections of fresh mouse distal ilea (30–100 mg) were minced with surgical scissors in 500 µL of 0.5 M acetic acid with 10 mg/mL pepsin, and agitated (at 1000 rpm on a VWR microplate shaker) overnight at 4°C and tissue debris was removed, as previously described.[24] Collagen was measured by the Sircol assay for soluble collagen (Biocolor Ltd, Carrickfergus, UK), according to the manufacturer's instructions. Collagen concentrations in samples were determined by comparing them to the linear portion of a standard curve.

Cytokine measurements

Cytokine measurements were performed on clarified full-thickness ileal tissue homogenates from mice by ELISA. ELISA kits for mouse IL-4, IL-1β, and IL-6 were from BD Biosciences (Mississauga, ON). The mouse TGFβ1 ELISA kit was from eBioscience (San Diego, CA).

Immunohistochemistry for F4/80 and YVAD-FLICA staining

Macrophages were stained with F4/80 as described previously.[27] Tissue sections were photographed at ×40 magnification at 6 points in each of six stained sections separated by >50 µm and macrophages were counted by two individuals blinded to experimental condition. For detection of active caspase-1, F4/80-stained sections were co-stained with YVAD-FLICA immediately before counterstaining with Harris' Hematoxylin (ImmunoChemistry Technologies, Bloomington, MN, USA). Tissue sections were thoroughly rinsed and then stained with DAPI.[24]

Statistical analyses

One-way ANOVAs were performed using GraphPad Prism version 5 software (version 5; GraphPad Software, Inc, La Jolla CA). For multiple comparisons, the Bonferroni correction was applied. Differences were considered significant at $P < 0.05$.

ACKNOWLEDGEMENTS

L.M.S. is the recipient of a Canadian Association of Gastroenterology/Crohn's and Colitis Canada/CIHR New Investigator Salary Award and is a Biomedical Scholar of the Michael Smith Foundation for Health Research. This work was supported by an operating grant awarded to LMS by the Canadian Institutes of Health Research (MOP-133607).

AUTHOR CONTRIBUTIONS

Y.L., T.S.S., and L.M.S. conceived of the study, designed the experiments, and analyzed the data. Y.L., J.P.S., and S.C.M. performed the experiments. L.M.S. supervised all aspects of the study. Y.L., T.S.S., and L.M.S. prepared and wrote the paper with contributions from all authors.

ADDITIONAL INFORMATION

The online version of this article (https://doi.org/10.1038/s41385-019-0191-z) contains supplementary material, which is available to authorized users.

Competing interests: The authors declare no competing interests.

Publisher's note: Springer Nature remains neutral with regard to jurisdictional claims in published maps and institutional affiliations.

REFERENCES

1. Molodecky, N. A. et al. Increasing incidence and prevalence of the inflammatory bowel diseases with time, based on systematic review. *Gastroenterology* **142**, 46–54 e42 (2012).
2. Xavier, R. J. & Podolsky, D. K. Unravelling the pathogenesis of inflammatory bowel disease. *Nature* **448**, 427–434 (2007).
3. Solberg, I. C. et al. Clinical course in Crohn's disease: results of a Norwegian population-based ten-year follow-up study. *Clin. Gastroenterol. Hepatol.* **5**, 1430–1438 (2007).
4. Lewis, R. T. & Maron, D. J. Efficacy and complications of surgery for Crohn's disease. *Gastroenterol. Hepatol. (N. Y)* **6**, 587–596 (2010).
5. Chang, C. W. et al. Intestinal stricture in Crohn's disease. *Intest. Res.* **13**, 19–26 (2015).
6. Wynn, T. A. Common and unique mechanisms regulate fibrosis in various fibroproliferative diseases. *J. Clin. Investig.* **117**, 524–529 (2007).
7. Speca, S., Giusti, I., Rieder, F. & Latella, G. Cellular and molecular mechanisms of intestinal fibrosis. *World J. Gastroenterol.* **18**, 3635–3661 (2012).
8. Hazlewood, G. S. et al. Comparative effectiveness of immunosuppressants and biologics for inducing and maintaining remission in Crohn's disease: a network meta-analysis. *Gastroenterology* **148**, 344–354 e345 (2015). quiz e314-345.
9. Cosnes, J. et al. Factors affecting outcomes in Crohn's disease over 15 years. *Gut* **61**, 1140–1145 (2012).
10. Govani, S. M., Stidham, R. W. & Higgins, P. D. How early to take arms against a sea of troubles? The case for aggressive early therapy in Crohn's disease to prevent fibrotic intestinal strictures. *J. Crohns Colitis* **7**, 923–927 (2013).
11. Lichtenstein, G. R. Comprehensive review: antitumor necrosis factor agents in inflammatory bowel disease and factors implicated in treatment response. *Ther. Adv. Gastroenterol.* **6**, 269–293 (2013).
12. de Bruyn, J. R. et al. Intestinal fibrosis is associated with lack of response to Infliximab therapy in Crohn's disease. *PloS ONE* **13**, e0190999 (2018).
13. Day, A. S. & Burgess, L. Exclusive enteral nutrition and induction of remission of active Crohn's disease in children. *Expert Rev. Clin. Immunol.* **9**, 375–383 (2013).
14. Hawkins, P. T. & Stephens, L. R. PI3K signalling in inflammation. *Biochim. et. Biophys. acta* **1851**, 882–897 (2015).

15. Dobranowski P., Sly L. M. SHIP negatively regulates type II immune responses in mast cells and macrophages. *J. Leukocyte Biol.* **103**, 1053–1064 (2018).
16. Guo, H., Samarakoon, A., Vanhaesebroeck, B. & Malarkannan, S. The p110 delta of PI3K plays a critical role in NK cell terminal maturation and cytokine/chemokine generation. *J. Exp. Med.* **205**, 2419–2435 (2008).
17. Uno, J. K. et al. Altered macrophage function contributes to colitis in mice defective in the phosphoinositide-3 kinase subunit p110delta. *Gastroenterology* **139**, 1642–1653 (2010). 1653 e1641-1646.
18. Weisser, S. B. et al. Arginase activity in alternatively activated macrophages protects PI3Kp110delta deficient mice from dextran sodium sulfate induced intestinal inflammation. *Eur. J. Immunol.* **44**, 3353–3367 (2014).
19. McLarren, K. W. et al. SHIP-deficient mice develop spontaneous intestinal inflammation and arginase-dependent fibrosis. *Am. J. Pathol.* **179**, 180–188 (2011).
20. Kerr, W. G., Park, M. Y., Maubert, M. & Engelman, R. W. SHIP deficiency causes Crohn's disease-like ileitis. *Gut* **60**, 177–188 (2011).
21. Weisser, S. B. et al. Alternative activation of macrophages by IL-4 requires SHIP degradation. *Eur. J. Immunol.* **41**, 1742–1753 (2011).
22. Helgason, C. D. et al. Targeted disruption of SHIP leads to hemopoietic perturbations, lung pathology, and a shortened life span. *Genes Dev.* **12**, 1610–1620 (1998).
23. Satoh, T. et al. Identification of an atypical monocyte and committed progenitor involved in fibrosis. *Nature* **541**, 96–101 (2017).
24. Ngoh, E. N. et al. Activity of SHIP, which prevents expression of interleukin 1beta, is reduced in patients with Crohn's disease. *Gastroenterology* **150**, 465–476 (2016).
25. Lucas, C. L., Chandra, A., Nejentsev, S., Condliffe, A. M. & Okkenhaug, K. PI3Kdelta and primary immunodeficiencies. *Nat. Rev. Immunol.* **16**, 702–714 (2016).
26. Wills-Karp, M. & Finkelman, F. D. Untangling the complex web of IL-4- and IL-13-mediated signaling pathways. *Sci. Signal.* **1**, pe55 (2008).
27. Weisser, S. B. et al. SHIP-deficient, alternatively activated macrophages protect mice during DSS-induced colitis. *J. Leukoc. Biol.* **90**, 483–492 (2011).
28. Rieder, F. & Fiocchi, C. Intestinal fibrosis in IBD–a dynamic, multifactorial process. *Nat. Rev. Gastroenterol. Hepatol.* **6**, 228–235 (2009).
29. Gieseck, R. L. 3rd, Wilson, M. S. & Wynn, T. A. Type 2 immunity in tissue repair and fibrosis. *Nat. Rev. Immunol.* **18**, 62–76 (2018).
30. Bailey, J. R. et al. IL-13 promotes collagen accumulation in Crohn's disease fibrosis by down-regulation of fibroblast MMP synthesis: a role for innate lymphoid cells? *PloS ONE* **7**, e52332 (2012).
31. Pizarro, T. T. et al. SAMP1/YitFc mouse strain: a spontaneous model of Crohn's disease-like ileitis. *Inflamm. bowel Dis.* **17**, 2566–2584 (2011).
32. Bamias, G. et al. Proinflammatory effects of TH2 cytokines in a murine model of chronic small intestinal inflammation. *Gastroenterology* **128**, 654–666 (2005).
33. Bamias, G. et al. Commensal bacteria exacerbate intestinal inflammation but are not essential for the development of murine ileitis. *J. Immunol.* **178**, 1809–1818 (2007).
34. Mitra, A. et al. Dual mTOR inhibition is required to prevent TGF-beta-mediated fibrosis: implications for scleroderma. *J. Invest Dermatol* **135**, 2873–2876 (2015).
35. Kuroda, E. et al. SHIP represses Th2 skewing by inhibiting IL-4 production from basophils. *J. Immunol.* **186**, 323–332 (2011).
36. Rauh, M. J. et al. SHIP represses the generation of alternatively activated macrophages. *Immunity* **23**, 361–374 (2005).
37. Barron, L. & Wynn, T. A. Fibrosis is regulated by Th2 and Th17 responses and by dynamic interactions between fibroblasts and macrophages. *Am. J. Physiol. Gastrointest. Liver Physiol.* **300**, G723–G728 (2011).
38. Morris, S. M. Jr. Arginine metabolism: boundaries of our knowledge. *J. Nutr.* **137** (6Suppl 2), 1602S–1609S (2007).
39. Ali, K. et al. Inactivation of PI(3)K p110delta breaks regulatory T-cell-mediated immune tolerance to cancer. *Nature* **510**, 407–411 (2014).
40. Akula, M. K. et al. Control of the innate immune response by the mevalonate pathway. *Nat. Immunol.* **17**, 922–929 (2016).
41. Rieder, F., Fiocchi, C. & Rogler, G. Mechanisms, management, and treatment of fibrosis in patients with inflammatory bowel diseases. *Gastroenterology* **152**, 340–350 e346 (2017).
42. Park, M. Y. et al. Impaired T-cell survival promotes mucosal inflammatory disease in SHIP1-deficient mice. *Mucosal Immunol.* **7**, 1429–1439 (2014).
43. Soond, D. R. et al. PI3K p110delta regulates T-cell cytokine production during primary and secondary immune responses in mice and humans. *Blood* **115**, 2203–2213 (2010).
44. Condliffe, A. M. et al. Sequential activation of class IB and class IA PI3K is important for the primed respiratory burst of human but not murine neutrophils. *Blood* **106**, 1432–1440 (2005).
45. Ngoh, E. N. et al. The Crohn's disease-associated polymorphism in ATG16L1 (rs2241880) reduces SHIP gene expression and activity in human subjects. *Genes Immun.* **16**, 452–461 (2015).
46. Thia, K. T., Sandborn, W. J., Harmsen, W. S., Zinsmeister, A. R. & Loftus, E. V. Jr. Risk factors associated with progression to intestinal complications of Crohn's disease in a population-based cohort. *Gastroenterology* **139**, 1147–1155 (2010).
47. Rutgeerts, P. et al. Predictability of the postoperative course of Crohn's disease. *Gastroenterology* **99**, 956–963 (1990).
48. Kisseleva, T. & Brenner, D. A. Anti-fibrogenic strategies and the regression of fibrosis. *Best. Pr. Res Clin. Gastroenterol.* **25**, 305–317 (2011).
49. Yamamoto, T., Fazio, V. W. & Tekkis, P. P. Safety and efficacy of strictureplasty for Crohn's disease: a systematic review and meta-analysis. *Dis. Colon Rectum* **50**, 1968–1986 (2007).
50. Rogler, G. & Hausmann, M. Factors promoting development of fibrosis in Crohn's disease. *Front. Med.* **4**, 96 (2017).
51. Yang, Q., Modi, P., Newcomb, T., Queva, C. & Gandhi, V. Idelalisib: first-in-class PI3K delta inhibitor for the treatment of chronic lymphocytic leukemia, small lymphocytic leukemia, and follicular lymphoma. *Clin. Cancer Res* **21**, 1537–1542 (2015).
52. Somasundaram, R. et al. Analysis of SHIP1 expression and activity in Crohn's disease patients. *PloS ONE* **12**, e0182308 (2017).
53. Fernandes, S. et al. SHIP1 deficiency in inflammatory bowel disease is associated with severe crohn's disease and peripheral T cell reduction. *Front. Immunol.* **9**, 1100 (2018).
54. Okkenhaug, K. et al. Impaired B and T cell antigen receptor signaling in p110delta PI 3-kinase mutant mice. *Science* **297**, 1031–1034 (2002).